Semarak Engineering Journal

Journal homepage:
https://semarakilmu.my/index.php/sej/index
ISSN: 3036-0145

Synergistic Bio-Circular Renewable Energy Systems: Integrating Agricultural Waste-Derived Electrolytic Coolants for Next-Generation Photovoltaic Thermal (PV/T) Optimization in Tropical Regions

Singgih Dwi Prasetyo[1,*], Yuki Trisnoaji[1], Arya Kusumawardana[1], Misbahul Munir[1], Royb Fatkhur Rizal[1], Catur Harsito[2,3], Burhan Haji Shame[4], Zainal Arifin[2]

[1] Power Plant Engineering Technology, State University of Malang, Malang 65145, Indonesia
[2] Department of Mechanical Engineering, Universitas Sebelas Maret, Surakarta 57126, Indonesia
[3] Department of Mechanical, Computer, Industrial, and Management Engineering, Kangwon National University, Samcheok 25913, Korea
[4] The Ministry of Infrastructure, Communication and Transportation, Zanzibar 266, Tanzania

ARTICLE INFO

Article history:
Received 12 March 2026
Received in revised form 22 April 2026
Accepted 13 July 2026
Available online 8 August 2026

ABSTRACT

Tropical photovoltaic modules experience temperature-driven electrical losses, while large volumes of mature coconut water and other agricultural liquid residues remain underutilized. This study develops a bio-circular photovoltaic/thermal framework that treats a conditioned agricultural-waste liquid as a measurable engineering candidate rather than assuming that natural electrolytes inherently improve heat transfer. In this work, "stabilized bio-coolant" is an operational acceptance status: a traceable mature-coconut-water batch is screened and serially filtered, subjected to a validated thermal or membrane treatment, stored in an opaque closed system, and accepted only after 30-day microbial, pH, turbidity, viscosity, gas/phase-separation, and hydraulic-stability checks. A transparent evidence workflow combined literature review, systematic screening, bibliometric mapping, and quantitative outcome mapping of 32 validated publications. A reduced-order energy-balance model, a limited-data physics-informed neural network, a 50,000-run Monte Carlo simulation, and a side-by-side experimental protocol were then decision-coupled. At 1,000 W/m² and 20 g/s, the bio-coolant reduced module temperature by 11.89 °C and increased electrical power by 5.63% relative to the uncooled PV baseline. However, water remained the better coolant benchmark: total efficiency was 50.73% for the bio-coolant and 52.99% for water, a bio-coolant deficit of 2.26 percentage points. The physics-informed model achieved 0.21 °C RMSE and $R^2 = 0.998$, while uncertainty analysis yielded a median reduction of 7.14 °C and a 38.56% probability of meeting an 8 °C target. The coupled workflow generated two non-obvious findings: cooling efficacy relative to uncooled PV does not imply superiority to water, and weather, flow, and construction uncertainty can dominate modest fluid-property differences. The concept is therefore a conditional resource-substitution pathway, not a proven high-performance replacement for water; corrosion, microbial stability, pumping energy, and long-duration tropical field validation remain mandatory.

Keywords:
bio-circular economy; agricultural waste; electrolytic bio-coolant; photovoltaic/thermal system; physics-informed deep learning; Monte Carlo simulation

* *Corresponding author.*
E-mail address: singgih.prasetyo.fv@um.ac.id

https://doi.org/10.37934/sej.15.1.172198

1. Introduction

Photovoltaic/thermal (PV/T) collectors simultaneously recover electricity and useful heat from the same aperture. This hybrid architecture addresses a fundamental limitation of photovoltaic conversion: only part of the incident solar energy is converted into electricity, while the remainder increases module temperature and is subsequently rejected to the environment. Foundational reviews by Zondag [1] and Chow [2] found that liquid-based PV/T collectors can convert this otherwise detrimental heat into a useful thermal stream, provided that hydraulic design, absorber contact, external heat loss, and pumping energy are treated as coupled system variables.

The challenge is intensified in humid tropical regions, where high irradiance, warm ambient air, weak midday wind, and persistent moisture can raise module operating temperature and accelerate soiling, corrosion, and encapsulant degradation. For crystalline-silicon modules, electrical efficiency generally decreases approximately linearly with cell temperature over the normal operating range [3]. Faiman [4] further demonstrated that outdoor temperature prediction is governed by irradiance and wind-dependent heat-loss coefficients rather than by irradiance alone. Consequently, this manuscript uses two non-interchangeable comparators. The uncooled PV baseline determines whether active circulation provides a cooling and electrical benefit. In contrast, water PV/T determines whether the candidate bio-coolant is competitive as a working fluid under matched irradiance, geometry, mass flow, and pumping conditions. A positive gain relative to uncooled PV must not be interpreted as superiority relative to water.

Active water cooling and conventional PV/T collectors can suppress temperature and recover heat [5-9]. Nanofluids and phase-change materials have also produced high laboratory performance, including improved overall energy efficiency for silica/water coolant [10], high thermal efficiency for CuO/water collectors [11], and combined efficiencies above 80% for SiC-based systems tested under tropical conditions [12,13]. However, the reported outcomes are not directly comparable because the authors use different reference systems, nanoparticle concentrations, absorber geometries, mass flow rates, definitions of efficiency, and uncertainty procedures. Long-term colloidal stability, pump wear, occupational exposure, material recovery, and end-of-life handling also remain constraints for deployment [6,13-16].

A circular alternative is to valorize locally available agricultural liquid waste as a working fluid or as a precursor for engineered heat-transfer media. Coconut water contains water, sugars, amino acids, and dissolved mineral ions whose composition varies with cultivar and maturity [17,18]. Its density, viscosity, thermal conductivity, diffusivity, and specific heat are temperature dependent [19], while mature coconut water is mildly acidic and highly perishable [20]. Electrical and dielectric behavior confirms the presence of mobile ions [21], but electrical conductivity is not equivalent to thermal conductivity. Therefore, an “electrolytic” coolant should not be presumed superior. Here and throughout, “stabilized” is not used as a vague chemical descriptor; it is an operational status assigned only after the batch-specific conditioning and the 30-day acceptance protocol in Section 3.4 have been completed. Before that point, the material is referred to as a conditioned candidate bio-coolant.

The circular-bioeconomy rationale is nevertheless strong. Agro-industrial residues can be converted into useful materials and process streams, reducing disposal burdens and diversifying rural value chains [22]. The supplied concept draft proposed a 100 Wp module, an aluminum absorber, a copper serpentine, a 12 V pump, an ESP32 acquisition, and side-by-side tropical testing. It also proposed 8-12 °C cooling and 10-15% electrical gain. The latter relationship is thermodynamically favorable for ordinary crystalline silicon: an 8-12 °C reduction with a temperature coefficient near -0.4%/°C typically implies roughly 3-5% electrical gain, unless other mechanisms or a much hotter reference module are involved. This study retains the useful system concept but replaces unverified performance assumptions with transparent equations, uncertainty distributions, and falsifiable acceptance criteria.

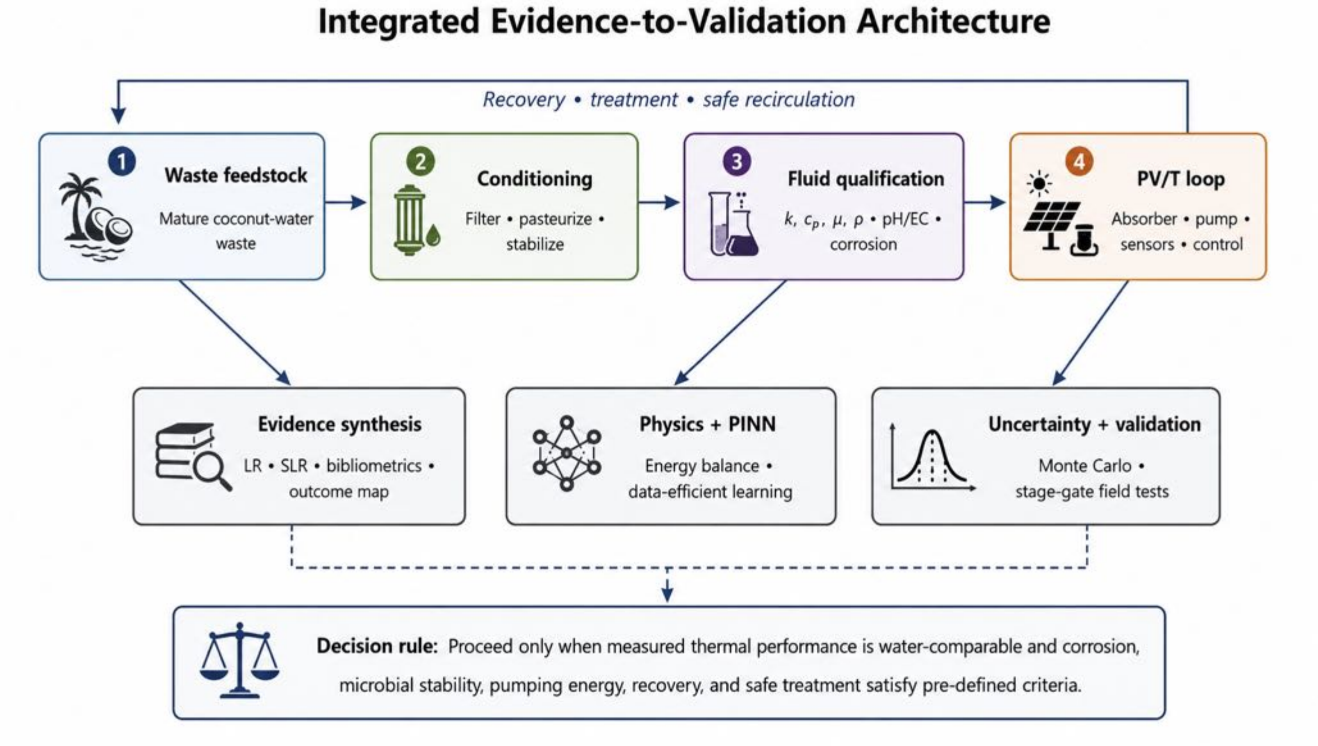

Fig. 1. Integrated evidence-to-validation framework for synergistic bio-circular PV/T optimization

Figure 1 defines the proposed system boundary. Agricultural waste is not considered a ready-made coolant; it undergoes conditioning and quality control before circulation. The layers are sequentially coupled rather than merely co-located: evidence synthesis defines comparator rules and property priors; fluid qualification converts a variable waste stream into measured inputs and uncertainty distributions; the reduced-order model supplies conservation equations and synthetic operating states; the PINN uses those constraints to regularize sparse-data prediction; Monte Carlo analysis converts point estimates into target probabilities; and field tests update the priors and stage-gate decisions. A circular feedback path requires recovery or treatment of spent fluid rather than uncontrolled discharge.

The research gap is the absence of a decision-coupled method that simultaneously (i) qualifies variable agricultural liquid waste as an auditable engineering fluid, (ii) prevents cross-comparator rhetoric when PV/T evidence is heterogeneous, (iii) embeds mass and energy conservation within a data-efficient surrogate, (iv) quantifies the probability of meeting thermal and electrical targets under tropical variability, and (v) converts those probabilities into a reproducible water-relative field decision. Accordingly, the objective is to develop and demonstrate this framework using mature coconut water waste as the reference feedstock. The contribution is not the number of tools assembled. It is the dependency structure among them, which produces findings that no single layer can provide: a coolant may deliver a meaningful gain relative to uncooled PV while remaining inferior to water; a nominal design target may have a low probability across realistic weather; and the largest deployment risks may arise from weather, hydraulic contact, stability, and lifecycle burden rather than ionic conductivity.

Table 1
Research questions and corresponding evidence streams

Research question	Primary method	Decision output
RQ1. What is established about liquid, nanofluid, and PCM cooling of PV/T systems?	LR and systematic evidence screening	Mechanisms, reported performance, limitations, and benchmark ranges
RQ2. Where is the interdisciplinary gap between agricultural-waste valorization and PV/T cooling?	Bibliometric-style keyword mapping	Theme clusters and weak links between circular bioeconomy, coolant qualification, and PV/T control
RQ3. Can an operationally stabilized coconut-water candidate offer a benefit over uncooled PV while approaching the matched-water benchmark?	Thermophysical screening and reduced-order simulation	Comparator-labeled temperature, electrical, thermal, and total-efficiency predictions
RQ4. Can limited labeled conservation laws augment data?	Physics-informed neural network (PINN)	Prediction error, R^2, and energy-residual error relative to a data-only ANN
RQ5. How robust are design targets under tropical variability?	Monte Carlo simulation and rank sensitivity	Target probabilities, uncertainty intervals, and dominant variables
RQ6. What evidence is required before field deployment?	Controlled experimental protocol	Acceptance criteria for performance, corrosion, microbes, pressure drop, and lifecycle handling

2. Comprehensive Literature Review

2.1 Bio-Circular PV/T System Boundaries

The supplied Bio-Circular Renewable Energy Systems evidence map organizes the field around five interacting domains: PV/T thermal management, agricultural-waste valorization, hybrid heat-transfer materials, physics-informed artificial intelligence, and environmental-economic deployment. A comprehensive review must distinguish integration at the system level from the mere co-location of technologies. In a genuinely bio-circular PV/T architecture, the waste stream has a defined origin, conditioning route, functional role, recovery pathway, and end-of-life destination; the recovered heat has an identified use; and the control system accounts for both performance and degradation. This boundary prevents a linear model in which agricultural waste is consumed as a disposable coolant.

Circular-bioeconomy literature supports cascade utilization rather than single-product conversion. Plant-derived residues contain water, minerals, carbohydrates, proteins, lignocellulose, and bioactive compounds that can be separated or converted through complementary biochemical and thermochemical routes [22,34-37]. For a liquid residue such as mature coconut water, the highest-value sequence may include recovery of food- or chemical-grade fractions where feasible, followed by controlled use of the rejected aqueous fraction as a technical fluid, and final treatment or recovery after circulation. For solid residues, pyrolysis and activation can generate biochar or porous carbon, while extraction and fermentation can produce chemicals and fuels. These pathways are related but not interchangeable: evidence that biomass-derived carbon improves a phase-change material does not prove that untreated biomass liquid is a suitable coolant.

2.2 Evolution of PV/T Cooling and Tropical Performance

PV/T research has progressed from air and water collectors to nanofluids, phase-change materials (PCM), heat pipes, radiative surfaces, and active hybrid control [1,2,5,6]. Water remains the reference liquid because of its high heat capacity, low viscosity, availability, and well-characterized behavior. Its limitations include freezing in some climates, corrosion when chemistry is uncontrolled, biological growth in open systems, and the opportunity cost of freshwater use. In tropical applications, freezing is unimportant, but elevated ambient temperatures, high humidity, low wind speeds, intense rainfall, salt exposure, and persistent soiling create demanding thermal and durability conditions [8,9,12,13,43]. Consequently, collector efficiency alone is insufficient; tropical suitability also depends on sealing, electrical insulation, rear-surface ventilation, corrosion resistance, and stable pump operation.

Nanofluids seek to raise thermal conductivity and convective heat transfer by dispersing particles such as SiO2, Al2O3, CuO, ZnO, or SiC in a base fluid. Experimental studies report substantial gains, but the magnitude depends on concentration, particle size, surfactant, sonication, channel geometry, flow regime, and comparator [10-16]. Recent reviews confirm that mono-, hybrid-, and ternary nanofluids can enhance PV/T electrical and thermal outputs, while also identifying sedimentation, agglomeration, increased viscosity, erosion, preparation costs, toxicity, and the lack of standardized stability tests as unresolved barriers [38,39]. Therefore, a bio-derived coolant should not be benchmarked only against the highest nanofluid result. It should first demonstrate reproducible performance relative to water at equal irradiance, mass flow, absorber geometry, and net pumping energy.

PCM integration addresses a different mechanism. Whereas a circulating fluid removes sensible heat, a PCM buffers temperature through latent heat storage. Nanofluid-PCM combinations can therefore be synergistic during short high-irradiance periods, but their benefits diminish after the PCM is fully melted unless night-time regeneration is effective [14-16]. Bio-based fatty-acid PCMs and biochar-supported composites potentially improve circularity, shape stability, and thermal conductivity, yet they add interfaces, mass, cost, flammability considerations, and lifecycle burdens. The literature consequently supports a staged comparison: uncooled PV, water PV/T, conditioned bio-coolant PV/T, and only then more complex coolant-PCM or biochar-PCM configurations.

2.3 Agricultural-Waste-Derived Electrolytic Coolants

Agricultural-waste-derived electrolytic coolants can be classified into three routes. The direct-liquid route uses an aqueous residue after clarification and stabilization. The reconstituted route extracts salts, organic acids, or biopolymers from waste and blends them into a controlled base fluid. The nanomaterial route converts solid waste into cellulose nanocrystals, carbonaceous particles, silica-rich ash, or metal-supported biochar, which is then dispersed in water or embedded in a PCM. The first route offers the lowest processing intensity but the highest biological and compositional variability. The second offers better formulation control but may lose the environmental advantage if extraction, purification, or additives are energy-intensive. The third can deliver high thermal conductivity or surface area, but it inherits the colloidal stability and safety issues of conventional nanofluids.

Coconut water is a technically relevant model feedstock because it is predominantly water but contains potassium, sodium, calcium, magnesium, chloride, phosphate, sugars, amino acids, and organic acids [17,18]. Its thermophysical properties vary with temperature and solids content [19], while maturity and storage alter pH, composition, and stability [20]. Dielectric and electrical measurements confirm ionic mobility [21], yet electrical conductivity cannot serve as a surrogate for thermal conductivity or the convective heat-transfer coefficient. Dissolved ions may slightly change density, heat capacity, boiling behavior, and corrosion potential, while sugars and suspended organic matter may increase viscosity, promote microbial growth, and form deposits. A credible literature-based formulation must therefore report thermal conductivity, specific heat, density, viscosity, pH, electrical conductivity, total dissolved solids, turbidity, microbial load, and corrosion behavior as independent variables.

The strongest conceptual advantage of a waste-derived liquid is not an assumed intrinsic heat-transfer superiority but resource substitution. A conditioned residue may reduce freshwater consumption or waste-treatment demand if collection, stabilization, replacement frequency, and final treatment are favorable. Conversely, repeated pasteurization, high preservative loading, frequent filter replacement, corrosion inhibitors, or short coolant life can eliminate the circular benefit. Integrated biorefinery studies emphasize that economic feasibility depends on feedstock logistics, year-round supply, co-products, process scale, and realistic capital and operating costs [34,37]. These findings support decentralized conditioning near coconut-processing centers rather than long-distance transport of a high-water-content feedstock.

2.4 Physics-Informed Learning and Adaptive Control

The digital layer identified in the source evidence map is most valuable when it links heterogeneous data to governing physics. Purely data-driven models can fit irradiance, temperature, flow, and power histories, but they may generate physically impossible states outside the training range. Physics-informed and physics-guided approaches incorporate solar geometry, temperature coefficients, energy balances, or residuals from differential equations into features, architectures, constraints, or loss functions [28,29,40,41]. Reviews classify hybrid PV models into physics-informed machine learning, optimized physical models, and physics-guided models [40]. Benchmark studies show that even relatively simple physical features can improve short-term forecasting and data efficiency [41].

For PV/T control, the principal state variables are module temperature, inlet and outlet coolant temperatures, irradiance, ambient temperature, wind speed, mass flow rate, and pump power. A physics-informed surrogate can estimate unmeasured heat fluxes, detect energy-balance violations, and optimize flow under sensor scarcity. Recent multi-scale PV forecasting work further demonstrates the feasibility of coupling numerical weather prediction with physics-informed neural networks [42]. Nevertheless, a high R2 value does not establish deployability. Models must be tested across wet and dry seasons, sensor drift, changing fluid properties, fouling, pump degradation, and unseen weather regimes. Uncertainty intervals and out-of-distribution detection are therefore necessary for safe adaptive control.

2.5 Bibliometric, Meta-Analytic, and Sustainability Evidence

The thematic structure in the source file is consistent with bibliometric studies of circular production and agricultural waste management: publication growth is concentrated around the circular economy, biomass conversion, pyrolysis, biorefineries, nanomaterials, and policy, while engineering studies of tropical deployment are less connected to social and governance research [35]. PV/T literature constitutes a mature technical cluster, whereas direct studies of agricultural liquid-waste coolant remain sparse. This asymmetry explains why a conventional meta-analysis of the complete topic is not yet defensible. Comparable effect sizes require common baselines, uncertainty estimates, flow normalization, and consistent definitions of electrical, thermal, exergy, and total efficiency. Where those conditions are absent, structured outcome mapping and subgroup-specific synthesis are more scientifically valid than a single pooled percentage.

Sustainability assessment must also extend beyond operational efficiency. Life-cycle and multi-criteria reviews show that agri-food waste technologies involve trade-offs among global warming potential, water use, eutrophication, toxicity, capital cost, rural employment, and supply reliability [44]. For the proposed coolant, the functional unit should include both delivered electricity and useful heat. In contrast, the counterfactual should include the existing fate of coconut-water waste and the water-based PV/T alternative. The system boundary should cover collection, filtration, stabilization, additives, pumping, component corrosion, fluid replacement, heat utilization, treatment, and discharge. Without these elements, a circularity claim risks shifting the burden from waste disposal to chemical use, equipment replacement, or contaminated effluent.

Additional contemporary evidence supports the revised system boundary, though it does not directly validate the coconut-water coolant. CFD analysis of water/Al2O3 PV/T collectors found that fin geometry significantly affected thermal and electrical conversion, whereas the tested fluid-concentration differences were not significant [45]. Experiments with passive fins likewise showed that geometry and arrangement materially affected PV temperature and electrical efficiency [46]. Water-spray experiments demonstrated that nozzle type and spray distribution altered cooling performance and efficiency [47]. A Central Java PV feasibility study showed that system architecture and cost structure can dominate adoption decisions [48], while spray-drying research on a biomass-derived liquid illustrated that a stability-enhancing process can impose substantial energy demand [49]. Together, these studies justify treating collector design, comparator choice, and stabilization burden as coupled variables rather than attributing performance solely to fluid identity.

Table 2
Comprehensive literature synthesis and implications for the proposed bio-circular PV/T framework

Literature domain	Established evidence	Critical unresolved issue	Response in this manuscript
Tropical PV reliability	High temperature and humidity reduce output and accelerate material degradation [3,4,8,9,43]	Matched outdoor baselines and long-duration durability are often absent	Side-by-side monitoring, weather-bin analysis, and durability stage gates
Water and conventional PV/T	Liquid cooling reliably lowers temperature and recovers useful heat [1,2,5-9]	Performance depends on absorber contact, flow, pump energy, and heat use	Water is retained as the engineering benchmark at equal hydraulic conditions
Nanofluid and PCM cooling	High laboratory thermal and combined efficiencies are reported [10-16,38,39]	Heterogeneous metrics, colloidal stability, toxicity, cost, and end-of-life handling	Outcome mapping without false pooling and a lower-complexity particle-free prototype
Agricultural-waste valorization	Cascade biorefineries can create materials, fuels, chemicals, and energy products [22,34-37]	Feedstock seasonality, logistics, scale-up, and co-product allocation	Decentralized feedstock qualification and explicit circular mass balance
Electrolytic liquid residues	Coconut water has measurable ionic and thermophysical properties [17-21]	Electrical conductivity is not proof of enhanced thermal performance; microbial and corrosion risks remain	Independent measurement of k, cp, rho, mu, pH, EC, microbes, fouling, and corrosion
Physics-informed AI	Physical priors improve data efficiency, interpretability, and robustness [28,29,40-42]	Simulation-to-field transfer, uncertainty, and sensor failure are under-tested	Energy-residual PINN, field calibration roadmap, and probabilistic thresholds
LCA, TEA, and governance	Circular technologies require environmental-economic trade-off assessment [35,37,44]	Optimistic boundaries can ignore additives, replacement, and waste treatment.	Functional-unit definition, net pump energy, treatment route, and stage-gated LCA/TEA

2.6 Integrated Research Gap and Testable Propositions

The comprehensive review yields five testable propositions. First, a conditioned agricultural liquid may provide a positive cooling benefit relative to uncooled PV while still underperforming water; both statements can be simultaneously true and must be reported with explicit comparators. Second, a batch may be considered stabilized only after a defined treatment route and time-resolved checks of microbial, physicochemical, and hydraulic acceptance, not merely because it has been filtered or stored. Third, feedstock variability, absorber contact, weather, and fouling are expected to influence long-term performance more strongly than electrical conductivity alone. Fourth, physics-informed learning should provide its greatest advantage under limited or partially missing field data, but only when energy residuals and predictive uncertainty are monitored. Fifth, the bio-circular pathway is advantageous only when water-relative performance, lifecycle treatment, component durability, and local waste-management credits outweigh the burdens of stabilization, pumping, and replacement. These propositions convert the review into falsifiable cross-layer decisions rather than a descriptive catalog.

3. Methodology
3.1 Review Design and Evidence Governance

The review component followed the PRISMA 2020 reporting logic [23], adapted for an engineering evidence-to-design study. The supplied Scopus-AI report was treated as a discovery map rather than as an authoritative bibliography because automated synthesis can contain citation or interpretation errors. Each included reference, therefore, required a verifiable title, venue, year, and either a DOI or an official standard record. Foundational PV/T and temperature-model papers published before the main search window were retained when they defined equations or benchmarking practices. Five reviewer-requested Scopus-indexed publications [45-49] were added during revision as targeted contextual triangulation. Because the original screening corpus had already been locked, they informed interpretation and method refinement. Still, they were not retroactively inserted into the n = 32 keyword network or the n = 11 quantitative outcome map.

As shown in Figure 2, 100 seed records from the supplied evidence map were supplemented with 28 publisher, DOI, and backward-search records. After 19 duplicate or overlapping records were removed, 109 titles and abstracts were screened. Forty-two records underwent full-text or complete metadata assessment, and 32 were retained in the validated evidence set. Eleven studies reported sufficiently explicit thermal, electrical, combined-efficiency, temperature-reduction, or stability outcomes for quantitative outcome mapping. The mapping deliberately avoided a single pooled effect where definitions were incompatible.

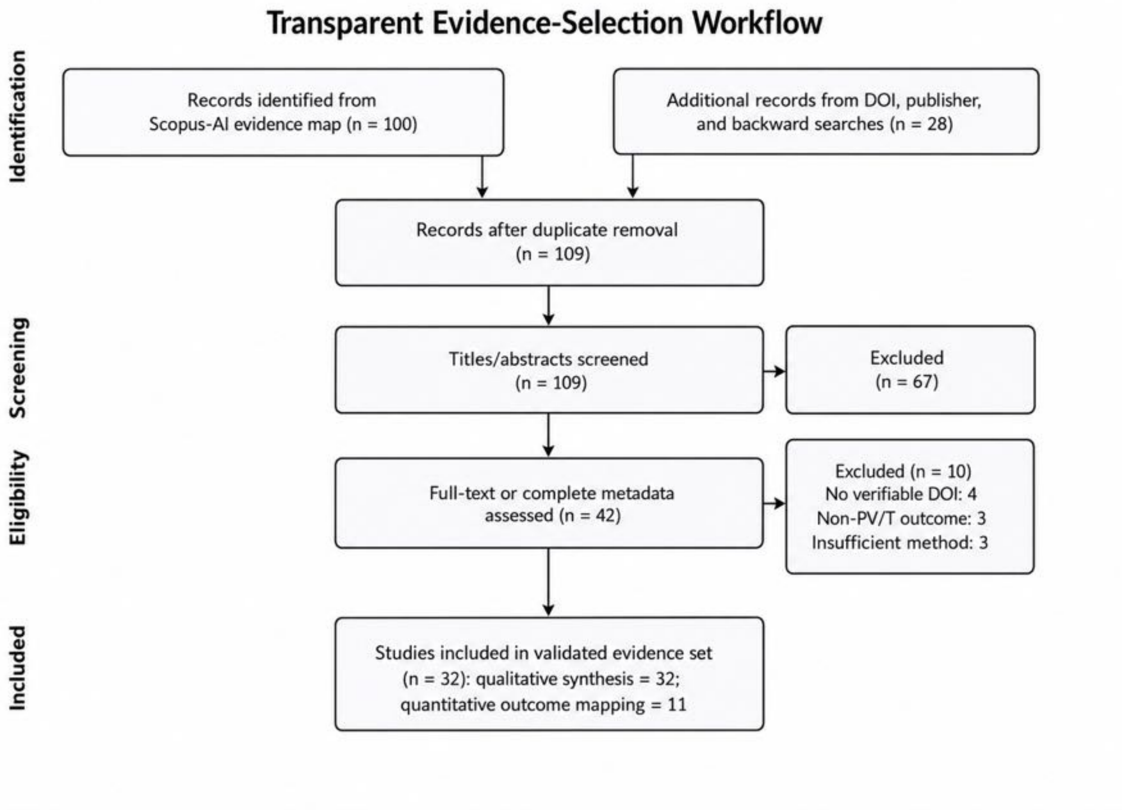

Fig. 2. Evidence-selection workflow used to construct the validated corpus

Table 3
Search logic, eligibility criteria, and quality controls

Element	Operational specification
Databases and sources	Publisher pages, DOI/Crossref-indexed records, Scopus-AI seed report, reference chaining, IEC and ISO standards
Core search concepts	("photovoltaic thermal" OR PVT OR PV/T) AND (cooling OR coolant OR nanofluid OR phase change material); combined with tropical, coconut water, agricultural waste, bio-coolant, physics-informed, deep learning, uncertainty, and Monte Carlo
Time scope	Primary technology evidence: 2014-July 2026; foundational PV/T and temperature models: earlier studies retained when methodologically essential
Inclusion	Peer-reviewed research/review or official standard; verifiable metadata; PV/PV-T thermal management, agricultural-waste fluid/material properties, circular bioeconomy, PINN, bibliometrics, or uncertainty method directly supporting the framework.
Exclusion	Unverifiable metadata; duplicated outcomes; no thermal/electrical relevance; unsupported promotional claims; absence of sufficient methodological description
Quality checks	Reference-system clarity; SI units; outcome definition; meteorological and flow conditions; uncertainty reporting; stability, corrosion, or environmental considerations; DOI validation
Synthesis rule	Narrative synthesis for mechanisms; frequency/co-occurrence mapping for themes; outcome mapping for heterogeneous performance metrics; no statistically pooled effect without a compatible denominator and variance

3.2 Bibliometric-Style Science Mapping

A reproducible science-mapping table was created from the 32 validated records using publication year, method, system, fluid/material, climate, and author keywords. Keyword variants were consolidated; for example, PVT and photovoltaic thermal were merged as PV/T, while physics-informed neural networks and physics-informed machine learning were grouped as physics-informed learning. Co-occurrence edges were created when two normalized terms appeared in the same record. Bibliometrix and VOSviewer provide established workflows for this type of analysis [24,25]; the present map is intentionally described as bibliometric-style because it is based on a curated, topic-specific evidence set rather than a complete database export.

Figure 3 shows a dense PV/T-nanofluid cluster associated with stability, PCM, and the tropical climate, while circular bioeconomy and agricultural waste form a separate cluster. Physics-informed learning connects strongly with forecasting and uncertainty but weakly with coolant formulation. This separation operationalizes the central gap: publications optimize thermal systems, valorize biomass, or develop AI models, but rarely integrate all three in a single qualification-and-control framework.

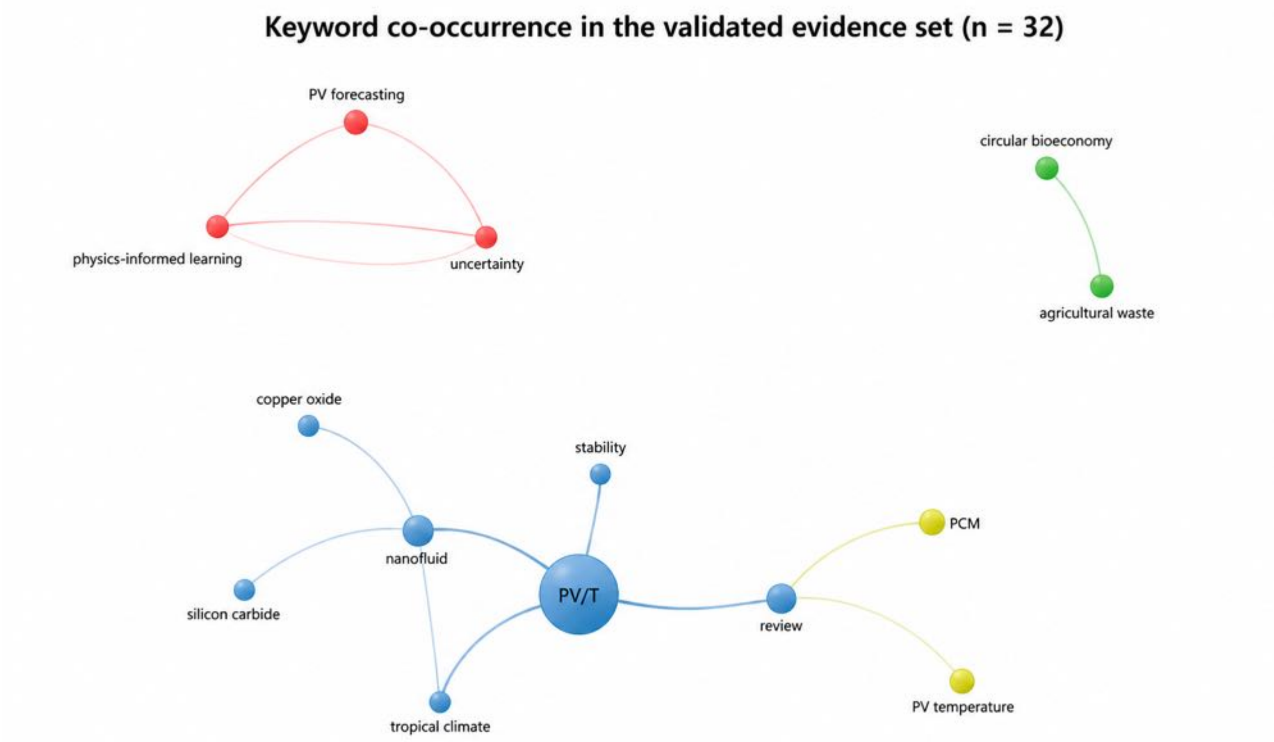

Fig. 3. Keyword co-occurrence network of the validated evidence set

3.3 Meta-Analytic Evidence Strategy

A conventional random-effects meta-analysis requires commensurate effects and within-study variances [26,27]. The screened PV/T literature did not meet this requirement. Some papers reported relative improvements over water, others reported absolute electrical or thermal efficiencies, and others reported exergy or total effectiveness relative to an uncooled PV module. A single pooled mean would therefore be numerically precise but scientifically misleading. The study instead used meta-analytic evidence principles: every result was encoded as outcome–comparator–condition, including irradiance, flow, geometry, and pumping boundary. Thus, the 5.63% electrical-power gain is defined only relative to uncooled PV, whereas the 50.73% versus 52.99% total-efficiency comparison is defined only between bio-coolant and water PV/T. These quantities answer different questions and are never combined into one superiority claim. A formal random-effects model is reserved for a future dataset with matched outcomes and reported standard errors.

Table 4
Representative validated PV/T cooling evidence and interpretation

Study	Configuration and conditions	Reported result	Use in this study
Sardarabadi et al. [10]	SiO_2/water, 1 and 3 wt%, experimental PV/T	At 3 wt%, overall energy efficiency increased 7.9% and thermal efficiency 12.8% versus water; total exergy increased 24.31% versus PV.	Benchmark for relative enhancement and the importance of comparator definition
Michael and Iniyan [11]	CuO/water in copper-sheet-laminated PV/T	High thermal performance, but electrical improvement is constrained by heat-exchanger effectiveness.	Evidence that better fluid properties do not compensate for poor thermal contact
Al-Shamani et al. [12]	SiO_2, TiO_2, and SiC in a rectangular absorber under tropical conditions	SiC case: 13.52% electrical and 81.73% combined efficiency at 1,000 W/m² and 0.17 kg/s	Tropical upper benchmark at a flow rate far above the proposed small-system design
Al-Waeli et al. [13]	3 wt% SiC/water PV/T	Thermal conductivity increased 8.2%; electrical efficiency improved 24.1% versus PV; overall effectiveness 88.9%	Shows high performance but also high solids concentration and specialized preparation
Sardarabadi et al. [14]	ZnO/water plus paraffin PCM	Average electrical output >13% above conventional PV; thermal output improved by nanofluid and PCM	Evidence for synergistic sensible and latent cooling
Al-Waeli et al. [15]	Nanofluid plus nano-PCM PV/T	Cell-temperature reduction near 30 °C; electrical efficiency increased from 7.1% to 13.7%; thermal efficiency 72%	Upper laboratory benchmark; not directly transferable to a particle-free waste-derived coolant
Al-Waeli et al. [16]	Nano-PCM/nanofluid technical-economic experiment	Electrical efficiency 13.7%, thermal efficiency 72%, 5-6-year payback under stated assumptions	Links technical outcome to pumping, cost, and utilization assumptions
This study recommends	Operationally stabilized coconut-water candidate; 100 Wp-class reduced-order model.	Versus uncooled PV: 11.89 °C reduction and 5.63% electrical gain; versus water: 50.73% versus 52.99% total efficiency	Demonstrates cooling efficacy but not water superiority; requires experimental validation

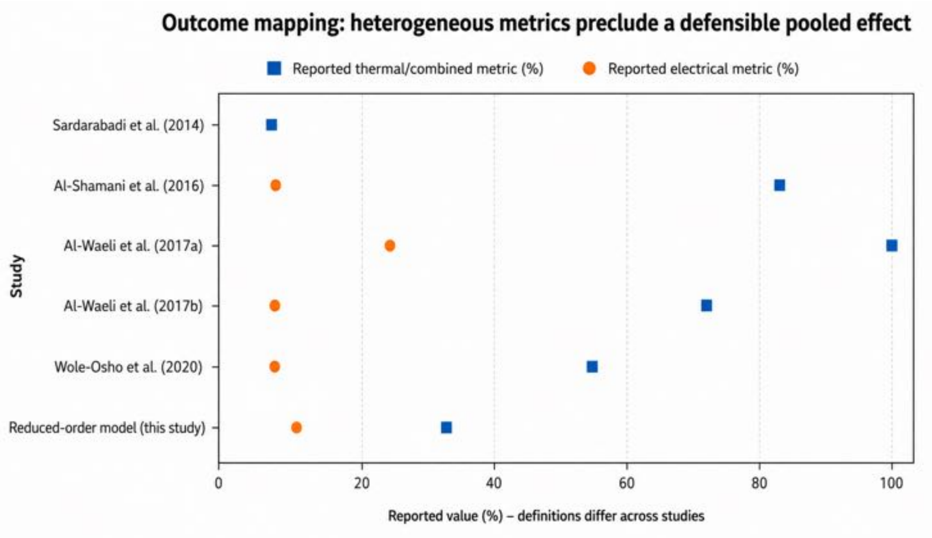

Fig. 4. Study-level outcome mapping; values are not pooled because reported definitions and comparators differ

3.4 Agricultural-Waste Coolant Preparation and Qualification

Mature coconut water rejected from food use is selected as the reference feedstock because it is abundant in tropical coconut-processing chains and contains naturally dissolved ions [17,18,21]. The formulation is a testable starting point, not a final recipe. The baseline conditioning sequence is: (i) document source, maturity, collection time, temperature, and visible contamination; (ii) remove shell and pulp with a 1 mm screen; (iii) clarify through 100-200 µm filtration followed by 5-20 µm final filtration; (iv) apply either a validated thermal pasteurization step or a membrane treatment in a closed hygienic path; and (v) store the batch in an opaque, closed container before circulation. Anaerobic fermentation is excluded because it can generate gas and organic acids, alter viscosity, and produce uncontrolled microbial metabolites. The baseline formulation contains no preservative, corrosion inhibitor, or antifreeze. Any later additive constitutes a separate formulation and must disclose chemical identity, concentration, effects on k, cp, ρ, µ, pH, and EC, as well as corrosion, toxicity, treatment, and lifecycle consequences.

Operational definition. A batch is classified as stabilized only after the conditioning sequence has been completed and the predeclared day 0, 7, 14, and 30 checks meet the requirements in Table 5. Stabilization in this manuscript means bounded change during the specified test window; it does not mean that the liquid is chemically inert, sterile indefinitely, compositionally identical across feedstock lots, or safe for unrestricted discharge. The treatment route, holding time, storage temperature, batch volume, and any additives must be reported to ensure the stability claim is reproducible and auditable.

Table 5
Proposed bio-coolant preparation, measurements, and pre-circulation acceptance limits

Stage/property	Method	Initial engineering criterion	Reason
Feedstock traceability	Record source, maturity, collection time, temperature, and visible contamination	Single documented batch per test block; compositional subsamples retained	Controls feedstock variability
Clarification	1 mm screen, 100-200 µm filtration, followed by 5-20 µm final filtration	No visible solids; turbidity reported; no filter bypass	Limits channel blockage and fouling
Stabilization	Validated pasteurization or membrane treatment in a closed path; opaque closed storage; baseline contains no preservative or antifreeze	Day 0, 7, 14, and 30 checks; no gas, foam, phase separation, or sediment; pH drift ≤0.20 and turbidity/viscosity drift ≤10%	Defines a reproducible operational status rather than an undefined chemical claim
pH and electrical conductivity	Calibrated pH and EC meters at 25 °C	pH 4.5-5.5 documented; EC measured as a batch fingerprint, not a proxy for thermal conductivity	Identifies acidity and ionic variability
Density and viscosity	Pycnometer/density meter and rotational or capillary viscometer at 25-60 °C	ρ = 1,000-1,035 kg/m³ and µ < 1.5 mPa·s as screening ranges	Sets flow and pumping requirements
Thermal conductivity and specific heat	Transient hot-wire/plane source and DSC or validated calorimetry	k and cp measured with uncertainty; nominal model ranges 0.50-0.66 W/m·K and 3.55-4.25 kJ/kg·K	Prevents unverified property assumptions
Corrosion compatibility	Copper and aluminum coupons, mass loss, microscopy, ion release	Corrosion rate no worse than deionized water control plus approved inhibitor system	Protects the absorber and piping
Microbial stability	Total plate count/ATP or validated equivalent at day 0, 7, 14, and 30, with batch and storage conditions reported	No persistent regrowth trend associated with odor, gas, pH/turbidity drift, biofilm, or pressure-drop increase	Controls biofilm and health risk
Hydraulic stability	Pressure drop and pump power over repeated heating cycles	<10% pressure-drop drift over test block; no sedimentation or foaming	Ensures repeatable operation

The thermophysical-property ranges in Table 5 are broad screening intervals derived from coconut-water studies and conservative engineering bounds [19-21]. They are not certified values for every feedstock. Only a batch that passes the complete conditioning and day 0, 7, 14, and 30 acceptance sequence is described as a stabilized bio-coolant; all other material is termed a conditioned candidate. The provisional stability gates are deliberately operational: no visible sedimentation, phase separation, foam, or gas generation; no persistent microbial-regrowth trend associated with odor, pH, turbidity, viscosity, or pressure-drop deterioration; pH drift within ±0.20 units; turbidity and viscosity drift within ±10%; and pressure-drop drift below 10% relative to day 0 under repeated heating cycles. These limits are engineering hypotheses for validation, not universal standards. Each batch must still be measured because sugar, minerals, solids, and pH vary with maturity and storage. Electrical conductivity is retained only as a batch fingerprint; the thermal model uses measured thermal conductivity, heat capacity, viscosity, and density directly.

3.5 PV/T Prototype and Field Protocol

The proposed apparatus consists of two matched 100 Wp-class monocrystalline modules mounted at the same tilt and azimuth. One module operates as an uncooled reference. The second is bonded to a 2 mm aluminum absorber that carries a 3/8-inch copper serpentine or an equivalent corrosion-compatible channel. Thermal interface material should have declared conductivity above 4 W/m·K and uniform bond-line thickness. A closed loop includes an insulated reservoir, a 12 V variable-speed pump, a calibrated flowmeter, a control valve, a particulate filter, temperature ports, and safe drain/recovery points.

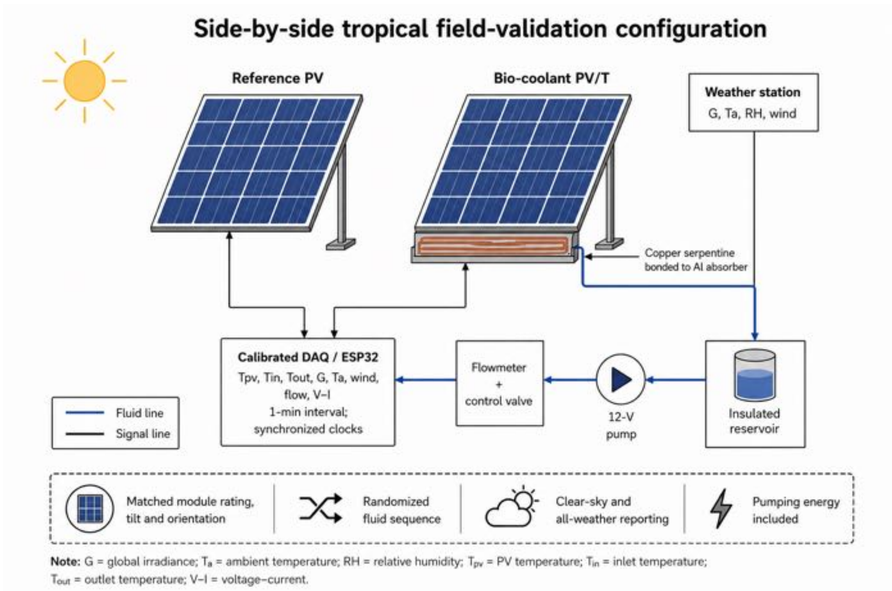

Fig. 5. Proposed side-by-side PV and bio-coolant PV/T experimental configuration

Figure 5 emphasizes matched exposure and synchronized measurement. Irradiance, ambient temperature, relative humidity, wind speed, module back-surface temperature at multiple points, fluid inlet/outlet temperature, mass flow, pressure drop, voltage, current, and pump power are logged at one-minute intervals. Electrical maximum-power tracking must be identical for both modules. The validation sequence uses three explicit states: uncooled PV for cooling benefit, water PV/T for coolant benchmarking, and bio-coolant PV/T for the candidate pathway. A randomized water/bio-coolant crossover on the same PV/T hardware separates fluid effects from construction tolerances. At least 7-14 clear days, supplemented by all-weather records, are required for preliminary validation; long-duration durability requires a substantially longer campaign.

3.6 Governing Physics and Reduced-Order Simulation

A steady-state control-volume model was implemented for design screening. The absorbed solar rate equals electrical conversion, external heat loss, and heat removed by the coolant. The external loss coefficient follows a Faiman-type wind relationship. The fluid-side conductance uses a number-of-transfer-units effectiveness term and an empirical dependence on flow rate and measured thermophysical properties. Recent CFD and experimental studies show that fin geometry, arrangement, and fluid-delivery design can materially affect PV/T and PV cooling outcomes [45-47]; therefore, fluid identity is not treated as the sole explanatory variable. This compact model is not a substitute for conjugate CFD. It provides transparent screening, exposes comparator logic, and supplies physically consistent synthetic states and conservation residuals for PINN evaluation.

$$\alpha GA = P_{\mathrm{el}} + h_{\mathrm{ext}} A\left(T_{\mathrm{pv}} - T_{\mathrm{a}}\right) + H\left(T_{\mathrm{pv}} - T_{\mathrm{in}}\right) \tag{1}$$

$$\eta_{\mathrm{el}} = \eta_{\mathrm{ref}}\left[1 + \beta\left(T_{\mathrm{pv}} - T_{\mathrm{ref}}\right)\right] \quad ; \quad P_{\mathrm{el}} = \eta_{\mathrm{el}} GA \tag{2}$$

$$h_{\mathrm{ext}} = U_0 + U_1 v \quad ; \quad \varepsilon = 1 - \exp\left[-\frac{UA}{\dot{m}c_p}\right] \quad ; \quad H = \varepsilon \dot{m} c_p \tag{3}$$

$$Q_{\mathrm{u}} = H\left(T_{\mathrm{pv}} - T_{\mathrm{in}}\right) = \dot{m}c_p(T_{\mathrm{out}} - T_{\mathrm{in}}) \tag{4}$$

$$\eta_{\mathrm{th}} = \frac{Q_{\mathrm{u}}}{GA} \quad ; \quad \eta_{\mathrm{tot}} = \eta_{\mathrm{el}} + \eta_{\mathrm{th}} \tag{5}$$

Here, α is the effective solar absorptance, G is the plane-of-array irradiance, A is the module area, β is the electrical temperature coefficient, v is the wind speed, and H is the effective fluid-side heat-removal conductance. The nominal module area was 0.67 m^2, η_{ref} = 0.18, β = -0.0041 K^{-1}, α = 0.90, and reference temperature 25 °C. The wind-loss relationship used U_0 = 20 W/m^2·K and U_1 = 6.84 W·s/m^3 as a conservative Faiman-type parameterization. The nominal bio-coolant used k = 0.575 W/m·K, cp = 3.92 kJ/kg·K, μ = 1.10 mPa·s, and ṁ = 0.020 kg/s.

Table 6
Nominal model parameters and their physical interpretation

Parameter	Nominal value	Role/source of uncertainty
Module area, A	0.67 m^2	100 Wp-class module geometry
Reference electrical efficiency, η_{ref}	0.180	Module technology and STC rating
Temperature coefficient, β	-0.0041 K^{-1}	Module datasheet and technology
Effective absorptance, α	0.90	Optical absorption and encapsulation
External loss, $U_0 + U_1 v$	20 + 6.84v W/m^2·K	Mounting, wind, humidity, rear ventilation
Reference clean-circuit UA	25 W/K at 0.020 kg/s	Bond quality, channel geometry, flow regime
Bio-coolant k	0.575 W/m·K	Feedstock composition and temperature
Bio-coolant cp	3.92 kJ/kg·K	Water/solids fraction and temperature
Bio-coolant μ	1.10 mPa·s	Sugar/solids, temperature, degradation
Fouling/contact multipliers	0.94 and 1.00 nominal	Surface aging, deposits, and bond-line nonuniformity

3.7 Physics-Informed Deep Learning

Physics-informed neural networks embed governing equations into the loss function, constraining predictions by conservation laws [28,29]. A ten-input multilayer perceptron received irradiance, ambient temperature, wind speed, mass flow, thermal conductivity, heat capacity, viscosity, fouling multiplier, contact multiplier, and inlet temperature. The output was module temperature. Only 240 labeled samples were used; 3,000 unlabeled collocation samples were used to supply the energy-balance residual. A data-only artificial neural network with the same architecture served as the comparator.

$$L_{\text{PINN}} = L_{\text{data}} + \lambda L_{\text{energy}} = \text{MSE}\left(\hat{T}_{\text{pv}}, T_{\text{pv}}\right) + \lambda \text{MSE}\left[\frac{R_E}{\alpha G A}\right] \tag{6}$$

$$R_E = \alpha G A - \hat{P}_{\text{el}} - h_{\text{ext}} A\left(\hat{T}_{\text{pv}} - T_{\text{a}}\right) - H\left(\hat{T}_{\text{pv}} - T_{\text{in}}\right) \tag{7}$$

Both networks used standardized inputs, three hidden layers with hyperbolic-tangent activation, Adam optimization, and a held-out test set. Performance was evaluated using RMSE, mean absolute error, R^2, and the RMSE of the unnormalized energy residual. The exercise is a reproducible in-silico benchmark: it demonstrates the value of physical regularization but does not constitute validation against field measurements.

3.8 Monte Carlo Uncertainty and Sensitivity

Monte Carlo simulation propagated uncertainty in climatic, fluid, hydraulic, and construction parameters through Eqs. (1)-(5). The method follows the general principle of sampling input distributions and evaluating the resulting output distribution [30,31]. Fifty thousand independent scenarios were generated. Distributions were selected as engineering priors rather than as universal tropical climatology; site-specific field data should replace them during deployment.

Table 7
Monte Carlo inputs for the tropical design-space analysis

Input	Distribution/range	Rationale
Irradiance, G	Triangular (350, 850, 1,100) W/m²	Daytime tropical operating envelope
Ambient temperature, Ta	Normal 31 ± 2.7 °C, truncated 24-39 °C	Warm-climate field variability
Wind speed, v	Triangular (0.25, 1.3, 4.0) m/s	Calm-to-breezy module ventilation
Mass flow, ṁ	Normal 0.020 ± 0.0045 kg/s, truncated 0.007-0.038	Pump/control and hydraulic variation
Thermal conductivity, k	Normal 0.575 ± 0.028 W/m·K, truncated 0.50-0.66	Batch and temperature variability
Specific heat, cp	Normal 3.92 ± 0.13 kJ/kg·K, truncated 3.55-4.25	Composition variability
Viscosity, μ	Lognormal about 1.10 mPa·s, truncated 0.70-2.00	Positive, skewed rheological uncertainty
Fouling multiplier	Uniform 0.80-1.00	Progressive heat-transfer degradation
Contact multiplier	Triangular 0.85, 0.97, 1.03	Bond-line and manufacturing variation
Inlet temperature	Ta + Uniform (0, 2.5) °C	Reservoir heat accumulation

Output probabilities were calculated for temperature-reduction thresholds of 8 °C and 10 °C, electrical-gain thresholds of 3% and 5%, and total efficiency. Spearman rank correlations were used as a monotonic global-sensitivity screen. A future field-calibrated model should replace rank correlation with variance-based indices when input dependence and non-monotonic effects are sufficiently characterized.

3.9 Experimental Statistics, Standards, and Reproducibility

PV monitoring and sensor classes should follow IEC 61724-1 [32], while thermal collector aspects should align with ISO 9806, where applicable [33]. Sensor calibrations, uncertainty budgets, missing-data rules, and exclusion of shading or maintenance intervals must be defined before analysis. Matched one-minute records can be aggregated to 5- or 15-minute intervals after quality control. All performance statements must retain an explicit comparator label: ΔTbio|uncooled and electrical gainbio|uncooled quantify cooling efficacy; Δηtotal, bio|water and the daily-yield gapbio|water quantify coolant competitiveness. The primary field analysis uses paired differences with meteorological covariates in a mixed-effects or generalized additive model. Pump electricity is subtracted from the net electrical benefit. Corrosion, microbial, physicochemical, and pressure-drop changes are analyzed as repeated measures. Cross-comparator wording is prohibited in the reporting template.

All simulation equations, distributions, random seeds, and derived figures were generated programmatically. The generated data represent model evidence, not experimental measurements. This distinction is maintained throughout the results and conclusion.

4. Results and Discussion

4.1 Evidence Synthesis and Research Gap

The validated corpus confirms that PV/T cooling is technically mature at the collector scale but not yet standardized at the evidence-synthesis level. Reported combined efficiencies span a broad range because thermal energy is valued differently, outlet-temperature targets differ, and some authors compare against water-cooled PV/T, while others compare against an uncooled PV module. Figure 4, therefore, maps study values without pooling. The reviewer-requested studies reinforce the same interpretation: fin geometry and arrangement can dominate the effects of tested fluid concentration [45,46]. At the same time, water-spray performance depends strongly on nozzle type and distribution [47]. The most transferable finding is therefore mechanistic rather than a universal percentage: module cooling depends on the full thermal-resistance network, fluid-delivery architecture, hydraulic point, and comparator. A nominally better fluid property cannot overcome poor absorber contact, inadequate area, or excessive pumping loss [10-16].

The agricultural-waste literature establishes the compositional and thermophysical variability of coconut water [17-21], while circular-bioeconomy literature supports its valorization in principle [22]. Yet none of the validated studies demonstrated long-duration coconut-water circulation through a copper/aluminum PV/T absorber with simultaneous electrical, thermal, corrosion, microbial, hydraulic, and lifecycle assessment. The specific novelty space is therefore not “using many methods.” It is the closure of this evidence-to-decision gap: a variable waste stream is assigned an operational stability status, translated into measured physical inputs, tested against conservation laws, propagated through uncertainty, and judged against a water-relative field gate. This chain prevents a positive uncooled-PV gain from being rhetorically recast as coolant superiority.

4.2 Deterministic Thermal-Electrical Performance

At the nominal peak condition of 1,000 W/m², ambient temperature 32.7 °C, wind near 1.5 m/s, and mass flow 0.020 kg/s, the reduced-order model predicted an uncooled module temperature of 57.87 °C. Water cooling reduced it by 12.65 °C to 45.22 °C, whereas the operationally stabilized bio-coolant reduced it by 11.89 °C to 45.98 °C. The bio-coolant was therefore 0.76 °C warmer than water under the matched condition. Its 5.63% electrical power gain is calculated relative to the uncooled PV module; it shows that active bio-coolant circulation can recover temperature-related electrical loss, but it does not demonstrate that the bio-coolant outperforms water.

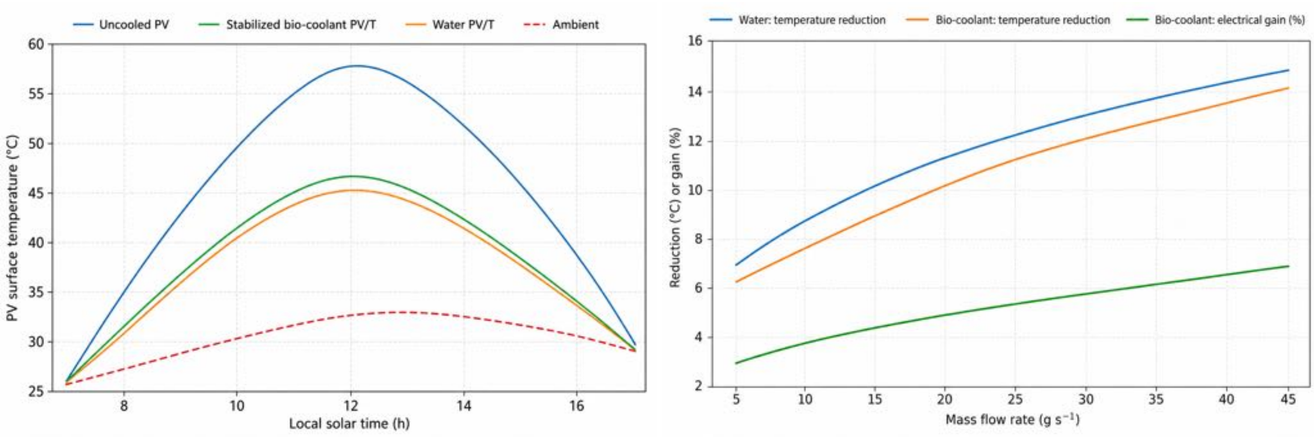

Fig. 6. Deterministic reduced-order results: (a) representative diurnal temperatures and (b) peak-condition flow-rate response

Figure 6(a) shows that both fluids suppress the midday temperature peak, with water retaining a modest advantage because its nominal heat capacity and conductivity are higher, and its viscosity is lower. The modeled peak total efficiency was 50.73% for the bio-coolant and 52.99% for water. Hence, the bio-coolant was 2.26 percentage points lower, equivalent to a 4.26% relative shortfall from the water benchmark. The bio-coolant delivered 16.45% electrical and 34.28% thermal efficiencies under peak conditions. Over the representative ten-hour day, electrical yields were 689.4 Wh for uncooled PV, 717.1 Wh for water PV/T, and 715.4 Wh for bio-coolant PV/T; the bio-coolant yield was 1.7 Wh, or 0.24%, below that of water PV/T. The defensible interpretation is therefore: beneficial relative to uncooled PV, near but inferior to water under the nominal assumptions, and potentially relevant only as a resource-substitution pathway if durability and lifecycle gates are satisfied.

Figure 6(b) reveals diminishing returns above approximately 20-30 g/s. Increased flow improves heat removal but also increases pump energy and can accelerate erosion or increase the risk of leakage. The optimal operating point must therefore maximize net exergy or net useful energy, not simply minimize module temperature. Adaptive control can exploit high flow during high-irradiance, low-wind periods and reduce flow when natural convection is sufficient.

4.3 Physics-Informed Surrogate Performance

The data-only ANN achieved a test RMSE of 0.50 °C, an MAE of 0.32 °C, and an R^2 of 0.9901. The PINN reduced RMSE to 0.21 °C and MAE to 0.11 °C, with R^2 = 0.9982. More importantly, the energy residual RMSE decreased from 17.51 W to 6.64 W. Physical regularization, therefore, improved both predictive accuracy and conservation consistency with limited labeled data.

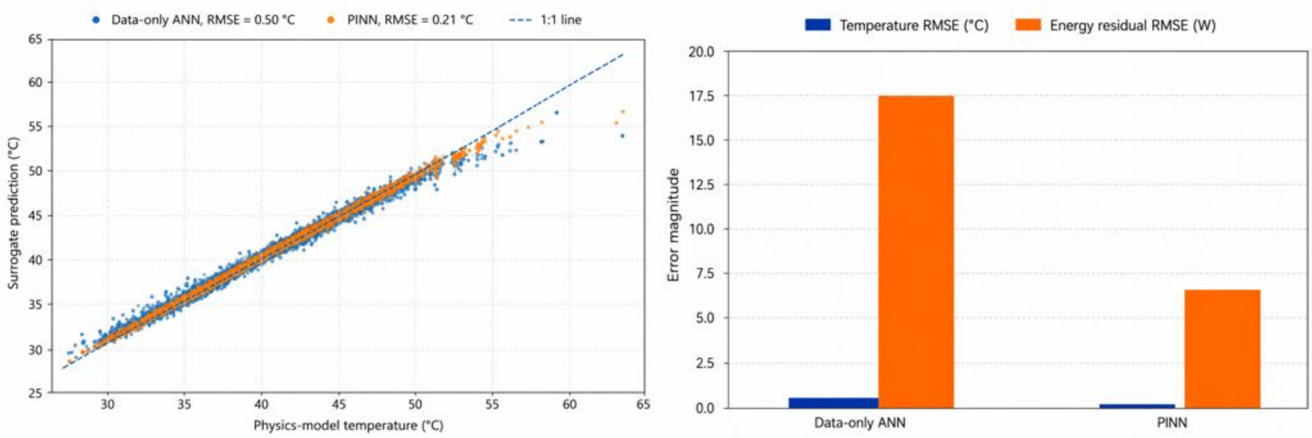

Fig. 7. Surrogate evaluation: (a) parity against the reduced-order physics model and (b) temperature and energy-residual errors

Figure 7 demonstrates why PINNs are attractive for tropical field deployment, where sensor failures and limited labeled experiments are common. However, the reported accuracy is against the same reduced-order physics used to generate training data. Real-field accuracy will be lower until the model is calibrated to account for spatial module temperatures, variable rear convection, thermal capacitance, changing fluid properties, and sensor uncertainty. The next stage should use transfer learning: pretrain on simulation, calibrate on water experiments, and then fine-tune on bio-coolant data while retaining energy residuals and uncertainty estimates.

4.4 Probabilistic Performance and Sensitivity

The Monte Carlo median temperature reduction was 7.14 °C, with a 5th-95th percentile interval of 3.55-12.58 °C. The probability of achieving at least 8 °C was 38.56%, and the probability of at least 10 °C was 18.53%. Median electrical gain was 3.24% (5th-95th percentile: 1.56-5.93%). The probabilities of achieving at least 3% and 5% electrical gain were 57.22% and 13.52%, respectively.

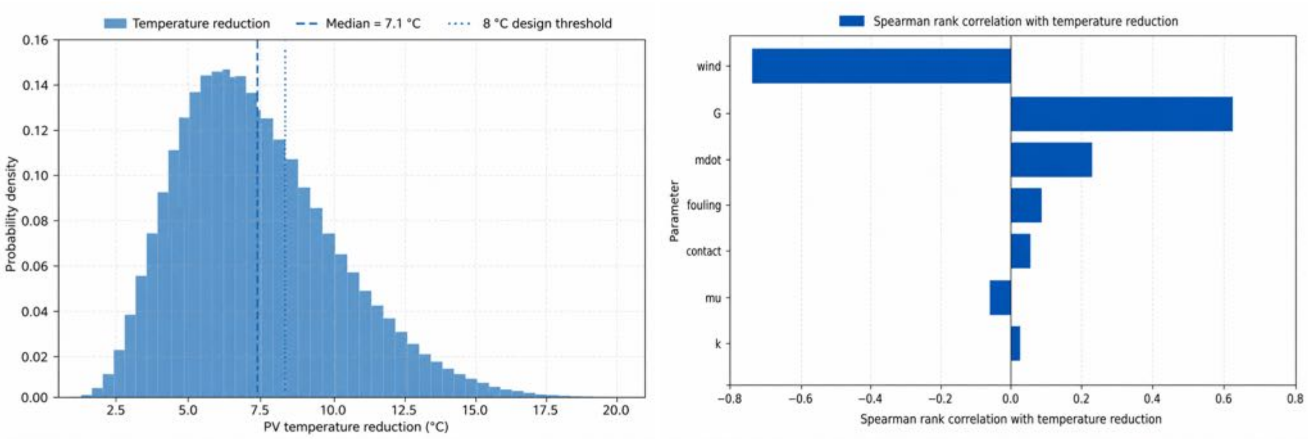

Fig. 8. Monte Carlo evidence: (a) probability distribution of temperature reduction and (b) rank sensitivity

The median total efficiency was 46.62%, with a 5th-95th percentile interval of 39.01-53.84%. Figure 8(b) identifies wind speed as the strongest negative driver of incremental cooling because high wind already cools the reference module. Irradiance is the strongest positive driver because more absorbed heat is available to remove. Mass flow has a smaller positive effect on temperature reduction but a stronger influence on thermal and total efficiency. Thermophysical-property uncertainty is secondary within the screened range. This is an emergent cross-layer result: literature review alone cannot rank these uncertainties, a deterministic model cannot expose their probability-weighted importance, and a PINN alone cannot define deployment risk. Their coupling shows that weather, hydraulic operation, and construction quality can dominate the modest fluid-property differences on which an "electrolytic superiority" narrative would otherwise rely.

These probabilities challenge deterministic target statements. The nominal design meets the 8-12 °C target at peak irradiance, yet only 38.56% of the broader sampled operating space reaches 8 °C. A credible field claim should therefore be conditional, for example: "median reduction under defined high-irradiance, low-wind bins," rather than a single all-weather value. Control optimization should target the meteorological bins in which active cooling yields the greatest net benefit.

Table 8
Integrated numerical results and interpretation

Metric	Data-only ANN / uncooled	PINN / bio-coolant	Interpretation
Peak module temperature	Uncooled PV: 57.87 °C	Bio-coolant PV/T: 45.98 °C	Versus uncooled: bio-coolant reduction 11.89 °C; water reduction 12.65 °C; bio-coolant remains 0.76 °C warmer than water
Peak electrical performance	Uncooled baseline	Electrical gain 5.63%	5.63% is explicitly relative to uncooled PV; it is not a water-comparison metric
Peak efficiencies	Water total efficiency: 52.99%	Electrical 16.45%; thermal 34.28%; total 50.73%	Bio-coolant is lower than water by 2.26 percentage points (4.26% relative shortfall)
Temperature prediction	ANN RMSE 0.50 °C; R^2 0.9901	PINN RMSE 0.21 °C; R^2 0.9982	Physics loss reduced prediction and conservation errors
Energy residual	ANN 17.51 W	PINN 6.64 W	Lower residual improves physical credibility
Monte Carlo temperature reduction	5th percentile 3.55 °C	Median 7.14 °C; 95th percentile 12.58 °C	$P(\Delta T \geq 8\ °C) = 38.56\%$
Monte Carlo electrical gain	5th percentile 1.56%	Median 3.24%; 95th percentile 5.93%	$P(\text{gain} \geq 5\%) = 13.52\%$

4.5 Experimental Acceptance Criteria and Falsifiability

A circular-energy concept is credible only if it can fail predefined tests. Table 9 converts the model into decision criteria and separates three claims: cooling efficacy relative to uncooled PV, coolant competitiveness relative to water, and circular advantage relative to the existing waste-management and water-use counterfactuals. Almost any circulating liquid may satisfy the first claim. Adoption requires that the second and third claims be supported simultaneously under equal hydraulic conditions and net pumping power, with an operationally stable batch that does not damage copper or aluminum and has a defensible treatment or recovery route.

Table 9
Proposed stage-gate criteria for laboratory and tropical field validation

Gate	Minimum evidence	Provisional pass criterion
G1 - Fluid qualification	Traceability plus replicated k, cp, μ, ρ, pH, EC, turbidity, and microbial measurements over 25-60 °C and days 0-30	Only a batch that passes all conditioning and stability limits is considered stabilized; otherwise, it remains a conditioned candidate.
G2 - Material compatibility	Copper/aluminum coupon tests and ion-release analysis	Corrosion not statistically worse than water control after inhibitor/lining strategy; no pitting or deposit layer
G3 - Hydraulic stability	Repeated thermal cycles with pressure-drop and pump-power logging	<10% pressure-drop drift and no blockage, foam, leakage, or filter overload
G4 - Thermal performance	Randomized water-versus-bio-coolant crossover at equal mass flow	Mean useful heat and module temperature within 5% of water at equal flow and pump power, or a quantified and explicitly justified resource trade-off
G5 - Net electrical performance	Matched PV reference; MPPT and pump electricity included	Positive net electrical gain in predefined high-benefit weather bins
G6 - Model validation	Out-of-sample comparison of reduced-order model and PINN with field data	Temperature RMSE <2 °C and no systematic energy-balance bias after calibration
G7 - Durability	Minimum 30-day pilot followed by seasonal testing	Stable pH, microbes, thermal properties, corrosion rate, and heat-transfer coefficient
G8 - Circularity and safety	Mass balance, treatment route, LCA/TEA boundary, worker, and discharge assessment	Documented recovery/treatment; no burden shifting relative to water and conventional coolant

The proposed "within 5% of water" criterion recognizes that adopting bio-coolant may be justified by waste reduction, local availability, or avoided treatment costs, even when thermal performance is slightly lower. Conversely, a small thermal advantage does not justify adoption if corrosion, microbial control, additive use, or disposal results in a greater environmental burden. The importance of system architecture and cost structure in PV feasibility [48], together with the substantial energy that can accompany biomass-liquid stabilization processes such as spray drying [49], reinforces the need to count conditioning energy rather than treating "stabilized" as cost-free. Lifecycle assessment and techno-economic analysis must therefore use measured replacement intervals, pumping energy, treatment requirements, and recovered heat utilization rather than optimistic laboratory assumptions.

Table 10
Decision coupling and knowledge generated by the integrated architecture

Coupled layer	Output passed forward	The individual layer does not solve the problem	Emergent knowledge or decision
Evidence governance	Comparator ontology, benchmark ranges, and property priors	A literature review can identify heterogeneity, but cannot test this candidate	Separates the benefit versus uncooled PV from competitiveness versus water
Fluid qualification	Measured k, cp, ρ, μ, pH, EC, stability, corrosion, and uncertainty distributions	A physics model otherwise assumes a generic and falsely stable fluid	Defines when the term stabilized is earned and when reformulation is required
Reduced physics + PINN	Energy residual, sparse-data surrogate, and violation checks	A data-only model can fit sparse data while violating conservation; a reduced model cannot adapt to field drift	Improves in-silico accuracy and physical consistency while retaining a field-calibration path
Monte Carlo + sensitivity	Target probabilities and ranked drivers	A nominal model hides target fragility and cannot prioritize uncertainty reduction.	Shows $P(\Delta T \geq 8\ °C) = 38.56\%$ and that weather/flow/contact can dominate fluid-property differences
Field + LCA/TEA gates	Water-relative pass/fail result, replacement burden, and treatment route	Thermal performance alone cannot establish a circular or economic advantage	Proceed only if near-water performance, durability, safety, and burden-shifting criteria are jointly satisfied

Table 10 makes the claimed synergy explicit. Each layer produces an output that constrains the next layer and can send a failed design backward for reformulation. The architecture, therefore, decides that a stand-alone literature review, deterministic model, data-only network, or uncertainty analysis cannot, on its own, determine whether a specifically qualified waste-derived batch is sufficiently close to water, sufficiently stable, and sufficiently circular to justify field deployment.

4.6 Limitations and Research Roadmap

The study has five principal limitations. First, the numerical results derive from a reduced-order model and should not be interpreted as measured prototype performance. Second, the bibliometric map is based on a validated thematic corpus rather than a complete export from Scopus or Web of Science; the five reviewer-requested references were contextual additions after corpus closure. Third, the heterogeneous PV/T literature did not permit a defensible pooled meta-analytic estimate of the effect. Fourth, the coconut-water property ranges do not capture every cultivar, maturity stage, storage history, or conditioning route. Fifth, the proposed 30-day stability limits are provisional engineering gates and have not yet been validated by microbial challenge tests, corrosion campaigns, or long-duration circulation.

The recommended roadmap is sequential and feedback-controlled. Stage 1 validates the conditioning route and assigns or rejects the stabilized-batch status through physicochemical, microbial, corrosion, and hydraulic tests. Stage 2 validates water operation and identifies the actual UA, external-loss coefficients, sensor uncertainty, and pump curve. Stage 3 performs randomized water/bio-coolant crossover tests using the explicit comparator template. Stage 4 calibrates the PINN and Monte Carlo distributions with field data and re-estimates the probability of meeting the water-relative gate. Stage 5 conducts long-duration durability, lifecycle, and economic assessment. Failure at any stage returns the formulation or hardware to the preceding layer; only after all gates should the system progress toward community-scale demonstration in coconut-producing tropical regions.

5. Conclusions

This study developed a comparator-aware evidence-to-validation framework to evaluate a candidate agricultural-waste-derived coolant for tropical PV/T systems. The validated literature confirms that active liquid cooling, nanofluids, and PCM hybrids can improve PV/T performance, but reported values are too heterogeneous for indiscriminate pooling. Coconut water provides a locally available ionic feedstock with a documented composition and temperature-dependent thermophysical properties; however, ionic conductivity alone does not confer enhanced heat transfer. The term stabilized bio-coolant is therefore restricted to a batch that has passed the specified filtration, thermal or membrane treatment, closed storage, and the 30-day microbial, physicochemical, and hydraulic acceptance sequence.

The reduced-order model predicted that the operationally stabilized bio-coolant would reduce peak module temperature by 11.89 °C and increase electrical power by 5.63% relative to uncooled PV at 1,000 W/m² and 20 g/s. Against the relevant coolant benchmark, however, it remained inferior to water: total efficiency was 50.73% versus 52.99%, a deficit of 2.26 percentage points, and representative daily electrical yield was 0.24% lower. Physics-informed learning reduced the temperature RMSE from 0.50 °C to 0.21 °C and improved energy conservation in the in silico benchmark. Monte Carlo analysis showed a median temperature reduction of 7.14 °C and only a 38.56% probability of meeting an 8 °C all-condition threshold, demonstrating that a favorable nominal result is not a robust all-weather superiority claim.

The principal novelty is not the mere aggregation of literature review, bibliometric mapping, reduced-order modeling, PINN regularization, Monte Carlo analysis, and field planning. It is the decision-coupled flow of information among those layers: evidence defines comparator and property priors; qualification determines whether a batch earns the stabilized status; physics constrains sparse-data learning; uncertainty converts point predictions into pass probabilities; and water-relative field and lifecycle gates determine adoption. This coupling generated new knowledge that the individual tools could not produce independently: the same candidate can be beneficial relative to uncooled PV yet inferior to water; the nominal 11.89 °C result has only a 38.56% probability of exceeding 8 °C across the sampled design space; and weather, flow, and construction quality can dominate modest fluid-property variation. The concept is therefore technically plausible only as a conditional resource-substitution pathway. Publication-grade claims require measured properties, paired tropical field data, net pumping-energy accounting, corrosion and microbial stability, and lifecycle-safe recovery or treatment.

Acknowledgement

We want to express our gratitude to the State University of Malang for providing an outstanding educational environment and resources that facilitate innovative research in renewable energy. This research was funded by the State University of Malang through the Non-Tax Revenue (Non-APBN) funding source, under the Faculty of Vocational Studies for the Fiscal Year 2026. It was conducted under the Decentralized Research Scheme, Contract Number 14.4.32/UN32.10.2/LT/2026, and the Rector's Decree Number 13.4.278/UN32/KP/2026.

Conflict of Interest Statement
The authors declare that there is no conflict of interest regarding the publication of this paper.

Author Contributions Statement
The contributions of each author were vital to the successful completion of this research. Singgih Dwi Prasetyo led the project, developing the initial framework and coordinating the overall study, while also making significant contributions to the conceptual design and methodology. Yuki Trisnoaji assisted with data collection and analysis, helped set up experiments, and played a key role in reviewing relevant literature and drafting sections of the paper. Arya Kusumawardana was instrumental in modeling the energy balance and conducting numerical simulations, and also participated in interpreting and discussing the results. Misbahul Munir supported the research by validating the data, helped develop the neural network model, and contributed to manuscript preparation. Royb Fatkhur Rizal conducted Monte Carlo simulations and analyzed uncertainty, focusing specifically on the bio-coolant's performance. Catur Harsito provided mechanical engineering expertise and contributed to discussions regarding the practical implications of the findings. Burhan Haji Shame offered insights into agricultural aspects. It helped relate the findings to real-world applications in tropical regions. At the same time, Zainal Arifin focused on the research design and provided critical feedback on the manuscript, particularly regarding its implications for the circular economy. All authors have read and approved the final manuscript and agree with the order of authorship.

Data Availability Statement
All equations, parameter distributions, simulated datasets, and derived figures used in this manuscript are available from the corresponding author upon reasonable request. The numerical results are explicitly identified as simulation outputs. No experimental human or animal data were generated.

Ethics Statement
This study used published literature and engineering simulation and did not involve human participants, animals, or personally identifiable data. Institutional ethical approval was therefore not required. Future fieldwork must comply with

References
[1] Zondag, H. A. "Flat-plate PV-Thermal collectors and systems: A review." *Renewable and Sustainable Energy Reviews* 12, no. 4 (2008): 891–959. https://doi.org/10.1016/j.rser.2005.12.012.
[2] Chow, T. T. "A review on photovoltaic/thermal hybrid solar technology." *Applied Energy* 87, no. 2 (2010): 365–79. https://doi.org/10.1016/j.apenergy.2009.06.037.
[3] Skoplaki, E., and J. A. Palyvos. "On the temperature dependence of photovoltaic module electrical performance: A review of efficiency/power correlations." *Solar Energy* 83, no. 5 (2009): 614–24. https://doi.org/10.1016/j.solener.2008.10.008.
[4] Faiman, David. "Assessing the outdoor operating temperature of photovoltaic modules." *Progress in Photovoltaics: Research and Applications* 16, no. 4 (2008): 307–15. https://doi.org/10.1002/pip.813.
[5] Michael, Jee Joe, S. Iniyan, and Ranko Goic. "Flat plate solar photovoltaic-thermal (PV/T) systems: A reference guide." *Renewable and Sustainable Energy Reviews* 51 (2015): 62–88. https://doi.org/10.1016/j.rser.2015.06.022.
[6] Al-Waeli, Ali H. A., Kamaruzzaman Sopian, Hussein A. Kazem, and Miqdam T. Chaichan. "Photovoltaic/thermal (PV/T) systems: Status and future prospects." *Renewable and Sustainable Energy Reviews* 77 (2017): 109–30. https://doi.org/10.1016/j.rser.2017.03.126.

[7] Teo, H. G., P. S. Lee, and M. N. A. Hawlader. "An active cooling system for photovoltaic modules." *Applied Energy* 90, no. 1 (2012): 309–15. https://doi.org/10.1016/j.apenergy.2011.01.017.
[8] Dubey, Swapnil, and Andrew A. O. Tay. "Testing of two different types of photovoltaic-thermal modules with heat flow pattern under tropical climatic conditions." *Energy for Sustainable Development* 17, no. 1 (2013): 1–12. https://doi.org/10.1016/j.esd.2012.09.001.
[9] Nahar, Afroza, M. Hasanuzzaman, and N. A. Rahim. "Numerical and experimental investigation on the performance of a photovoltaic thermal collector with parallel plate flow channel under different operating conditions in Malaysia." *Solar Energy* 144 (2017): 517–28. https://doi.org/10.1016/j.solener.2017.01.041.
[10] Sardarabadi, Mohammad, Mohammad Passandideh-Fard, and Saeed Zeinali Heris. "Experimental investigation of the effects of silica/water nanofluid on PV/T (photovoltaic thermal units)." *Energy* 66 (2014): 264–72. https://doi.org/10.1016/j.energy.2014.01.102.
[11] Michael, Jee Joe, and S. Iniyan. "Performance analysis of a copper sheet laminated photovoltaic thermal collector using copper oxide-water nanofluid." *Solar Energy* 119 (2015): 439–51. https://doi.org/10.1016/j.solener.2015.06.028.
[12] Al-Shamani, Ali Najah, Kamaruzzaman Sopian, Sohif Mat, Hasan A. Hasan, Abed M. Abed, and M. H. Ruslan. "Experimental studies of rectangular tube absorber photovoltaic thermal collector with various types of nanofluids under the tropical climate conditions." *Energy Conversion and Management* 124 (2016): 528–42. https://doi.org/10.1016/j.enconman.2016.07.052.
[13] Al-Waeli, Ali H. A., Kamaruzzaman Sopian, Miqdam T. Chaichan, Hussein A. Kazem, Husam Abdulrasool Hasan, and Ali Najah Al-Shamani. "An experimental investigation of SiC nanofluid as a base-fluid for a photovoltaic thermal PV/T system." *Energy Conversion and Management* 142 (2017): 547–58. https://doi.org/10.1016/j.enconman.2017.03.076.
[14] Sardarabadi, Mohammad, Mohammad Passandideh-Fard, and S. Zeinali Heris. "Experimental study of using both ZnO/water nanofluid and phase change material in photovoltaic thermal systems." *Solar Energy Materials and Solar Cells* 161 (2017): 62–69. https://doi.org/10.1016/j.solmat.2016.11.032.
[15] Al-Waeli, Ali H. A., Kamaruzzaman Sopian, Miqdam T. Chaichan, Hussein A. Kazem, Adnan Ibrahim, Sohif Mat, and Mohd Hafidz Ruslan. "Evaluation of the nanofluid and nano-PCM based photovoltaic thermal system: An experimental study." *Energy Conversion and Management* 151 (2017): 693–708. https://doi.org/10.1016/j.enconman.2017.09.032.
[16] Al-Waeli, Ali H. A., Hussein A. Kazem, Miqdam T. Chaichan, and Kamaruzzaman Sopian. "Experimental investigation of using nano-PCM/nanofluid on a photovoltaic thermal system: Technical and economic study." *Thermal Science and Engineering Progress* 11 (2019): 213–30. https://doi.org/10.1016/j.tsep.2019.04.002.
[17] Yong, Jean W. H., Liya Ge, Yan Fei Ng, and Swee Ngin Tan. "The chemical composition and biological properties of coconut (Cocos nucifera L.) water." *Molecules* 14, no. 12 (2009): 5144–64. https://doi.org/10.3390/molecules14125144.
[18] Prades, Alexia, Manuel Dornier, Nafissatou Diop, and Jean-Pierre Pain. "Coconut water uses, composition and properties: A review." *Fruits* 67, no. 2 (2012): 87–107. https://doi.org/10.1051/fruits/2012002.
[19] Fontan, Rafael Costa Ilhéu, Leandro Soares Santos, Renata Cristina Ferreira Bonomo, Alana Rocha Lemos, Raquel Prates Ribeiro, and Cristiane Martins Veloso. "Thermophysical properties of coconut water affected by temperature." *Journal of Food Process Engineering* 32, no. 3 (2009): 382–97. https://doi.org/10.1111/j.1745-4530.2007.00222.x.
[20] Appaiah, P., L. Sunil, P. K. Prasanth Kumar, and A. G. Gopala Krishna. "Physico-chemical characteristics and stability aspects of coconut water and kernel at different stages of maturity." *Journal of Food Science and Technology* 52, no. 8 (2015): 5196–5203. https://doi.org/10.1007/s13197-014-1559-4.
[21] Shah, N. S., P. S. Shah, and V. A. Rana. "Dielectric and electrical properties of coconut water and distilled water in the frequency range 20 Hz to 2 MHz at different temperatures." *Ionics* 21, no. 12 (2015): 3217–22. https://doi.org/10.1007/s11581-015-1506-z.
[22] Yaashikaa, P. R., P. Senthil Kumar, and Sunita Varjani. "Valorization of agro-industrial wastes for biorefinery process and circular bioeconomy: A critical review." *Bioresource Technology* 343 (2022): 126126. https://doi.org/10.1016/j.biortech.2021.126126.
[23] Page, Matthew J., Joanne E. McKenzie, Patrick M. Bossuyt, Isabelle Boutron, Tammy C. Hoffmann, Cynthia D. Mulrow, et al. "The PRISMA 2020 statement: An updated guideline for reporting systematic reviews." *BMJ* 372 (2021): n71. https://doi.org/10.1136/bmj.n71.
[24] Aria, Massimo, and Corrado Cuccurullo. "Bibliometrix: An R-tool for comprehensive science mapping analysis." *Journal of Informetrics* 11, no. 4 (2017): 959–75. https://doi.org/10.1016/j.joi.2017.08.007.
[25] van Eck, Nees Jan, and Ludo Waltman. "Software survey: VOSviewer, a computer program for bibliometric mapping." *Scientometrics* 84, no. 2 (2010): 523–38. https://doi.org/10.1007/s11192-009-0146-3.

[26] DerSimonian, Rebecca, and Nan Laird. "Meta-analysis in clinical trials." *Controlled Clinical Trials* 7, no. 3 (1986): 177–88. https://doi.org/10.1016/0197-2456(86)90046-2.
[27] Viechtbauer, Wolfgang. "Conducting meta-analyses in R with the metafor package." *Journal of Statistical Software* 36, no. 3 (2010): 1–48. https://doi.org/10.18637/jss.v036.i03.
[28] Raissi, Maziar, Paris Perdikaris, and George E. Karniadakis. "Physics-informed neural networks: A deep learning framework for solving forward and inverse problems involving nonlinear partial differential equations." *Journal of Computational Physics* 378 (2019): 686–707. https://doi.org/10.1016/j.jcp.2018.10.045.
[29] Karniadakis, George E., Ioannis G. Kevrekidis, Lu Lu, Paris Perdikaris, Sifan Wang, and Liu Yang. "Physics-informed machine learning." *Nature Reviews Physics* 3 (2021): 422–40. https://doi.org/10.1038/s42254-021-00314-5.
[30] Rubinstein, Reuven Y., and Dirk P. Kroese. *Simulation and the Monte Carlo Method*. 3rd ed. Hoboken: Wiley, 2016. https://doi.org/10.1002/9781118631980.
[31] Saltelli, Andrea, Marco Ratto, Terry Andres, Francesca Campolongo, Jessica Cariboni, Debora Gatelli, Michaela Saisana, and Stefano Tarantola. *Global Sensitivity Analysis: The Primer*. Chichester: Wiley, 2008. https://doi.org/10.1002/9780470725184.
[32] International Electrotechnical Commission. *IEC 61724-1:2021, Photovoltaic System Performance - Part 1: Monitoring*. Geneva: IEC, 2021.
[33] International Organization for Standardization. *ISO 9806:2017, Solar Energy - Solar Thermal Collectors - Test Methods*. Geneva: ISO, 2017.
[34] Jin, Qing, Liangcheng Yang, Nicholas Poe, and Haibo Huang. "Integrated processing of plant-derived waste to produce value-added products based on the biorefinery concept." *Trends in Food Science & Technology* 74 (2018): 119–31. https://doi.org/10.1016/j.tifs.2018.02.014.
[35] Duque-Acevedo, Monica, Luis J. Belmonte-Urena, Natalia Yakovleva, and Francisco Camacho-Ferre. "Analysis of the circular economic production models and their approach in agriculture and agricultural waste biomass management." *International Journal of Environmental Research and Public Health* 17, no. 24 (2020): 9549. https://doi.org/10.3390/ijerph17249549.
[36] Foong, Shin Ying, Rock Keey Liew, Yafeng Yang, Yoke Wang Cheng, Peter Nai Yuh Yek, Wan Adibah Wan Mahari, et al. "Valorization of biomass waste to engineered activated biochar by microwave pyrolysis: Progress, challenges, and future directions." *Chemical Engineering Journal* 389 (2020): 124401. https://doi.org/10.1016/j.cej.2020.124401.
[37] Manhongo, Tariro T., Annie F. A. Chimphango, Patricia Thornley, and Mirjam Roder. "Current status and opportunities for fruit processing waste biorefineries." *Renewable and Sustainable Energy Reviews* 155 (2022): 111823. https://doi.org/10.1016/j.rser.2021.111823.
[38] Venkateswarlu, Kavati, K. P. V. Krishna Varma, and Uday Kumar Nutakki. "Synthesis, characterization and application of mono-, hybrid and ternary nanofluids in hybrid photovoltaic thermal (PV/T) solar systems: A review." *Journal of the Brazilian Society of Mechanical Sciences and Engineering* 44 (2022): 550. https://doi.org/10.1007/s40430-022-03864-6.
[39] Madhi, Hussain, Sattar Aljabair, and Ahmed A. Imran. "A review of photovoltaic/thermal system cooled using mono and hybrid nanofluids." *International Journal of Thermofluids* 22 (2024): 100679. https://doi.org/10.1016/j.ijft.2024.100679.
[40] de Oliveira Santos, Leticia, Tarek AlSkaif, Giovanni Cordeiro Barroso, and Paulo Cesar Marques de Carvalho. "Photovoltaic power estimation and forecast models integrating physics and machine learning: A review on hybrid techniques." *Solar Energy* 284 (2024): 113044. https://doi.org/10.1016/j.solener.2024.113044.
[41] Vazquez Pombo, Daniel, Peder Bacher, Charalampos Ziras, Henrik W. Bindner, Sergiu V. Spataru, and Poul E. Sorensen. "Benchmarking physics-informed machine learning-based short term PV-power forecasting tools." *Energy Reports* 8 (2022): 6512–20. https://doi.org/10.1016/j.egyr.2022.05.006.
[42] Zhang, Fei, Xingcai Li, Zifa Wang, Yunyun Wen, Xuyang Zhou, Zichen Wu, et al. "MIPV-NWP-PINNs V1.0: Development of a multi-scale photovoltaic power forecasting framework integrating numerical weather prediction with physics-informed neural networks." *Geoscientific Model Development* 19 (2026): 4999–5017. https://doi.org/10.5194/gmd-19-4999-2026.
[43] Ogbomo, Osarumen O., Emeka H. Amalu, N. N. Ekere, and P. O. Olagbegi. "A review of photovoltaic module technologies for increased performance in tropical climate." *Renewable and Sustainable Energy Reviews* 75 (2017): 1225–38. https://doi.org/10.1016/j.rser.2016.11.109.
[44] Romero-Perdomo, Felipe, and Miguel Angel Gonzalez-Curbelo. "Integrating multi-criteria techniques in life-cycle tools for the circular bioeconomy transition of agri-food waste biomass: A systematic review." *Sustainability* 15, no. 6 (2023): 5026. https://doi.org/10.3390/su15065026.
[45] Prasetyo, Singgih Dwi, Zainal Arifin, Aditya Rio Prabowo, and Eko Prasetya Budiana. "Examining Various Finned Collector Geometries in the Water/Al2O3 Based PV/T System: An Analysis Using Computational Fluid Dynamics

Simulation." *International Journal of Heat and Technology* 42, no. 3 (2024): 851–64. https://doi.org/10.18280/ijht.420314.

[46] Basyar, Khoirul, Zainal Arifin, Dominicus Danardono Dwi Prija Tjahjana, and Singgih Dwi Prasetyo. "Analysis of the Impact of Different Fin Configurations as Passive Coolants on Photovoltaic Performance." *International Journal of Heat and Technology* 42, no. 6 (2024): 2115–24. https://doi.org/10.18280/ijht.420630.

[47] Wibowo, Santiko, Zainal Arifin, Rendy Adhi Rachmanto, Dwi Aries Himawanto, and Singgih Dwi Prasetyo. "Optimization of Photovoltaic Performance Using a Water Spray Cooling System with Different Nozzle Types." *International Journal of Computational Methods and Experimental Measurements* 12, no. 1 (2024): 9–19. https://doi.org/10.18280/ijcmem.120102.

[48] Arifin, Zainal, Marshima Mohd Rosli, Yudin Joko Prasojo, Noval Fattah Alfaiz, Singgih Dwi Prasetyo, and Windi Mulyani. "Economic Feasibility Investigation of On-Grid and Off-Grid Solar Photovoltaic System Installation in Central Java." *International Journal of Energy Production and Management* 8, no. 3 (2023): 169–75. https://doi.org/10.18280/ijepm.080305.

[49] Prasetyo, Singgih Dwi, Catur Harsito, Sutanto, and Suyitno. "Energy Consumption of Spray Dryer Machine for Producing Red Natural Powder Dye and Its Stability." *AIP Conference Proceedings* 2097, no. 1 (2019): 030076. https://doi.org/10.1063/1.5098251.